Geomechanics and Engineering, *Vol. 33, No. 4 (2023) 353-367*
https://doi.org/10.12989/gae.2023.33.4.353

Numerical investigation of the effect of impact on the rockfall protective embankment reinforced with geogrid

Mohammad Reza Abroshan[a] and Majid Noorian-Bidgoli*

Department of Mining Engineering, Faculty of Engineering, University of Kashan, Kashan, Iran

(*Received October 28, 2022, Revised March 8, 2023, Accepted March 20, 2023*)

Abstract. The construction of a protective embankment is a suitable strategy to stop and control high-energy rock blocks' impacts during the rockfall phenomenon. In this paper, based on the discrete element numerical method, by modeling an existing embankment reinforced with geogrid, its stability status under the impact of a rock block with two types of low and high kinetic energy, namely 2402 and 4180 kJ, respectively, has been investigated. The modeling results show that the use of geogrid has caused the displacement in the front and back of the embankment to decrease by more than 30%. In this case, the reinforced embankment has stopped the rock block earlier. The displacements obtained from the DEM modeling are compared with the displacements measured from an actual practical experiment to evaluate the results' validity. Comparison between the results shows that the displacement values are close together, while the maximum percentage error in previous studies by an analytical method and the finite element method was 76.4% and 36.6%, respectively. Therefore, the obtained results indicate the discrete numerical method's high ability compared to other numerical and analytical methods to simulate and design the geogrid-reinforced soil embankment under natural disasters such as rockfall with a minor error.

Keywords: discrete element method (DEM); geogrid; numerical modeling; protective embankment; rockfall; YADE

1. Introduction

Rockfall is a destructive phenomenon in high areas such as mountains, hills, and slopes. When it happens, one or more pieces of rock, due to generally natural and unnatural factors, are separated from the main substrate and fall downstream. The natural factors usually include weathering, earthquake, wind, storm, rainfall, flood, and melting of snow and ice, and the unnatural factors include explosion and ground vibration (Ouyang *et al.* 2019). This phenomenon can occur under various mechanisms such as sliding, toppling, or falling concerning the ground conditions. In each of these cases, the occurrence of rockfall, in addition to financial losses caused by interruptions in road and rail transportation systems, damage to the natural resources, facilities, structures, and vehicles, can even lead to fatalities (Crosta and Agliardi 2004). Therefore, in addition to accurate prediction and identification (Yan *et al.* 2023) of this phenomenon, it is necessary to be done preventive actions to prevent and spread this phenomenon.

These actions are classified into two categories, namely active and inactive actions (Peila *et al.* 2007). The active preventive actions are a set of operations to prevent the separation of rock pieces from its main body. For example, the use of rockbolt in areas with falling potential is one of these actions. But the passive preventive or mitigation actions are, in fact, the protection of the facilities, equipment, and structures after the occurrence of rockfall. In this regard, the protective embankment is a steep artificial slope used to stop the falling rock blocks. However, the impact of the rock blocks on the embankment may result in significant deformations, including compaction, slipping surfaces, and even the removal of constituent materials.

In general, concrete embankments, gabions, or pre-built concrete walls are also used to control rockfall. The most common types of these embankments are made of compacted soil (Paronuzzi 1989), huge rock blocks (Pasqualotto et al., 2004), compacted soil with one side made of gabions (Lambert *et al.* 2009), gabions (Wyllie and Norrish 1996), compacted soil reinforced with wooden and steel bars (Tissieres 1999), protective cushion (Zhu *et al.* 2018, Zhu *et al.* 2021), gabions and a reinforced structure (cellular sandwich structure) (Bourrier *et al.* 2010), compacted soil with two sides made of gabions (Simmons *et al.* 2009), reinforced ground and with an adsorbing mattress made of geotextile bags filled with sand (Geo Rock wall) (Yoshida 1999), reinforced ground with geotextile, geogrids or a metallic wire mesh (Burroughs *et al.* 1993, Lazzari *et al.* 1996, Pasqualotto *et al.* 2005, Oggeri *et al.* 2004, Peila and Ronco 2009). In most cases, protective embankments are large soil structures with the cross-sectional shape of trapezoid made perpendicular to the slope, which have a height between 3 to 25 m and a length of several hundred meters (Peckover and Kerr 1977, Maegawa *et al.* 2011). These embankments are suitable for controlling rockfall with medium to very high kinetic energy (from a few hundred kilojoules to tens of megajoules). They are preferred to wire mesh for impacts

*Corresponding author, Ph.D.
E-mail: noriyan@kashanu.ac.ir
[a]Ph.D.Student

ISSN: 2005-307X (Print), 2092-6219 (Online)

with a kinetic energy of more than 5000 kJ (Descourdes 1997). Their advantages include low maintenance costs and lack of visual effects on the environment. These types of embankments are often reinforced with geosynthetic materials such as geogrids. Geogrids are high-strength, orientated-polymer grid structures used to reinforce soils (Faisal Haji 1993). In this case, the geogrid is placed as reinforcement plates and box between the embankment layers and causes it to increase its tensile strength (Moradi *et al.* 2018, 2019).

Because the impact of rock blocks with high kinetic energy causes large and irreversible deformations in the embankment, the design of embankments that fully consider impact mechanisms is very complex. However, since the late 1980s, the design and use of reinforced structures to control high-energy rock blocks began (Lambert and Bourrier 2013). In this regard, analytical methods have been developed to solve the problems of high-impact collisions based on the balance of force and considering the impact of energy and energy absorbed by the soil. For instance, in a study conducted by Tissieres (1999), the limiting force of the rock block was compared to the shear strength of the embankment, assuming that the impact displaced a rigid portion of the embankment. Also, since numerical models' calibration is usually difficult in dynamic analysis, some designers prefer to use the more straightforward method to evaluate the reinforced embankment to protect against rockfall analytically (Peila *et al.* 2006).

One of the most well-known methods used for this purpose is proposed by Kar (1978). This method was obtained from the tests performed to investigate military projectiles' effect on the embankment and the amounts of projectile penetration into the soil and impact energy. This method often used to design embankments in the past (Paronuzzi 1989), but since the results are heavily influenced by the shape and speed of projectiles, which are very different from the rock blocks in the embankments, their application is difficult and uncertain for the rockfall problems.

Other methods that usually provide better results for calculating the maximum penetration depth of block in the embankment's front side are presented by Ronco *et al.* (2009). In this method, the penetration depth of the block (δ_p) is obtained by the maximum stop force of the block and 80 to 85% of the energy as follows.

$$\delta_p = \frac{(0.80:0.85).mv^2}{F_{\max}}[m] \quad (1)$$

Where, δ_P is the maximum displacement (m), m is the block mass (Kg), v is block velocity before impact (m/s), and $F_{\max}$ is the maximum force (N).

The coefficient selection is made according to the amount of energy, namely 0.85 is selected for the impact with energy less than 5000 kJ, and 0.80 for the impact with energy greater than 5000 kJ. In order to calculate the maximum stop force of the block, the developed formula as follows can be used based on the suggested models of Labiouse *et al*. (1996), which are obtained from the studies conducted in determining the thickness of the soil layer of the protective structures

$$F_{\max} = 1.765 M_E^{2/5} R^{1/5} ((0.80, 0.85) E_{kin})^{3/5} [KN] \quad (2)$$

Where, M_E is the elasticity coefficient of the soil (kN/m^2), R is the block radius (m), and E_{kin} is the kinetic energy of the block (kJ).

The maximum protrusion of the back side of the embankment (ξ) can also be achieved by modifying the block's kinetic energy and the friction force work in the layers' slide. In this regard, 0.15 is selected for the impact with energy less than 5000 kJ, and 0.20 for the impact with energy greater than 5000 kJ (Ronco *et al*. 2009). The results of this analysis show that the penetration depth in the front side of the embankment is 0.22 and 0.26 m, and the maximum protrusion of the back side of the embankment is about 0.04 and 0.06 m, due to the impact of the block with the kinetic energy of 2402 and 4180 kJ, respectively. Comparing the results of this method with the experimental test results shows that this method estimates lower penetration depth values than the experimental values.

However, due to the multiplicity of hypotheses and simplifications performed in this type of method, most of the available analytical methods presented, although easy to apply, are unreliable (Kister and Fontana 2011, Lambert and Kister 2017). In most of these methods, the slip of layers directly impacted by the block is not evaluated correctly. In the following, some researchers have tried to analyze granular materials' behavior (Pichler *et al.* 2005) and embankments (Burroughs et al., 1993; Peila *et al.* 2002) using real-scale impact tests on soil layers. In a research work, to investigate the effect of geogrid use on the protective embankment behavior, the impact test of a concrete block to a reinforced embankment was carried out by Peila *et al.* (2007) in Meano near Trento (North-East of Italy). In fact, this test was conducted to investigate the behavior of reinforced embankment when throwing a block by a launcher with two types of energy, namely 2402 and 4180 kJ, to define the relevant parameters in the design and determine the level of energy that the structure in the safe conditions can absorb. The results of this study show that in the first test (low impact energy), the maximum penetration depth in the front and back sides of the embankment was about 0.6 m and 0.17 m, respectively. Also, in the second test (high impact energy), the maximum penetration depth in the front and back sides of the embankment was about 0.95 m and 0.8 m, respectively. However, generalizing these results to other structures and materials doesn't seem to make sense. Furthermore, mechanical properties, the thickness of material under the impact, and boundary conditions strongly affect the system's response (Calvetti 1998). On the other hand, these tests are usually time-consuming and very costly to perform.

Due to experimental tests' limitations, numerical methods have been used to simulate the rockfall to consider all parameters affecting the protective embankment impact.

These research works include; one-dimensional models (Cantarelli *et al.* 2008), two-dimensional (Peila *et al.* 1998), and three-dimensional using the finite element method (Cazzani *et al.* 2002, Peila *et al.* 2002, Volkwein 2005), the discrete element method (Bertrand *et al.* 2005, Plassiard *et al.* 2005, Watanabe *et al.* 2011, Effeindzourou *et al.* 2017,

Zhu *et al.* 2019, Pol and Gabrieli 2021, Zhu *et al.* 2021, Zhu *et al.* 2021), and the finite-discrete element method (Tran *et al.* 2015). In this regard, the use of continuous methods such as FEM to model the rockfall has been more (Ronco *et al.* 2009). For example, Peila *et al.* (2007) simulated a real test based on the finite element numerical method using ABAQUS software. In summary, the results of this study showed that due to the impact of the block with 2402 kJ kinetic energy, the penetration depth on the front side of the embankment was about 0.38 m. The maximum protrusion of the back side of the embankment was about 0.2 m. In contrast, with 4180 kJ kinetic energy, the block's penetration depth on the front side of the embankment was about 0.95 m, and the maximum protrusion of the back side was about 0.5 m.

However, in these methods, the movement of particles (material flow), slip of embankment surfaces, and collapse processes that can occur during impact are not well evaluated. Therefore, using discrete methods can achieve better results by explicitly displaying the discontinuous nature of the soil in reality. Of course, it should be noted that in these methods, the solution changes depending on the initial arrangement of the particles, and the number of particles needs to be reduced because it takes considerable computation time. Also, it is not easy to set the DEM model parameters. In such cases, it is often useful to combine the use of two discrete and continuum methods. For example, Meng *et al.* (2023) developed a rigid-block DEM mode for the mesoscale fracture simulation of concretelike material considering the relatively large time-step of the DEM. In some cases, by explicit modeling of soil using the discrete element method, limitations of continuous methods can be overcome. In this regard, the two-dimensional modeling of block impact to an embankment without reinforcement has been carried out to define the desired specifications of material, in which the embankment is modeled as a set of blocks (Plassiard and Donze 2009). After that, Plassiard and Donze (2010) investigated the effective parameters of block and parameters of the embankment without reinforcement, for the design optimization of rockfall embankments. Since the damage caused by the impact on the soil embankment, there is a need to investigate the performance/effectiveness of geogrid for reinforcement of rockfall protective embankment. The subject has not been investigated sufficiently by providing a validation based on real-scale experiments in previous research works to examine the effect of impact on the protective embankment reinforced.

The aim of this study is to develop a numerical model based on the discrete element method (DEM), using YADE as an open-source code, that in addition to being able to correctly model the behavior of protective soil embankment reinforced with geogrid against the impact of rock block, it can have an acceptable agreement with the results measured from a real scale test. For this purpose, by applying impact to the embankment in the model, the penetration depth in the front side of embankment and protrusion in its back side was determined. In the end, in order to validate the results obtained a comparison between the developed model and the existing analytical and another numerical finding is performed.

Table 1 Geotechnical parameters of reinforced protective embankment materials (Peila *et al*. 2007)

Material	Parameter	Unit	Value
Soil	Density	KN/m^3	21
	Young's modulus	MPa	150
	Poisson's ratio	-	0.3
	Internal friction angle	◦	34
	Cohesion	KPa	9
Geogrid	Tensile Young's modulus	MPa	250
	Internal friction angle between soil and geogrid	◦	35
	Tensile strength	KN/m	45

2. Methodology

The real-scale rockfall tests are challenging to manage and perform, so these tests mainly study a limited number of embankment geometry changes and impact energy. On the other hand, because practical tests require large equipment, which is very expensive and time-consuming, the number of tests is often limited in the design stage. Therefore, in the design stage, these tests' results can be used to develop numerical models that can predict reinforced embankments' behavior under different conditions and impacts with varying energy levels. Their results can adjust numerical models to predict the structure's behavior against impacts with varying energy levels. In this study, the numerical models of the unreinforced and reinforced embankments with geogrid have been made based on the data of a practical test on a real protective embankment.

2.1 Experimental test

In a research work, a real test was done by Peila et al. (2007) in Meano near Trento (North-East of Italy), to investigate the effect of impact on the rockfall protective embankment reinforced with geogrid. In fact, this test was conducted to investigate the behavior of reinforced embankment when throwing a block by a launcher with two types of energy, namely 2402 and 4180 KJ, to define the relevant parameters in the design and determine the level of energy that the structure in the safe conditions can absorb.

The schematic of this reinforced embankment used in this test is shown in Fig. 1. According to this figure, the height of embankment is 4.2 m, its crest width is 0.9 m, its length in the out of plane direction is 8 m, and both sides' angle is equal to 67°. The embankment is made of 7 layers of the same compacted soil that between each layer is a polymer geogrid sheet (dotted green line). The trajectory of the collision of the block is perpendicular to the front face of the embankment. It means that the block face is parallel with the embankment face at the time of impact. Also, the impact point is at the height of 3 m from the floor, exactly in the middle of the front face of the embankment, according to the condition of the practical test.

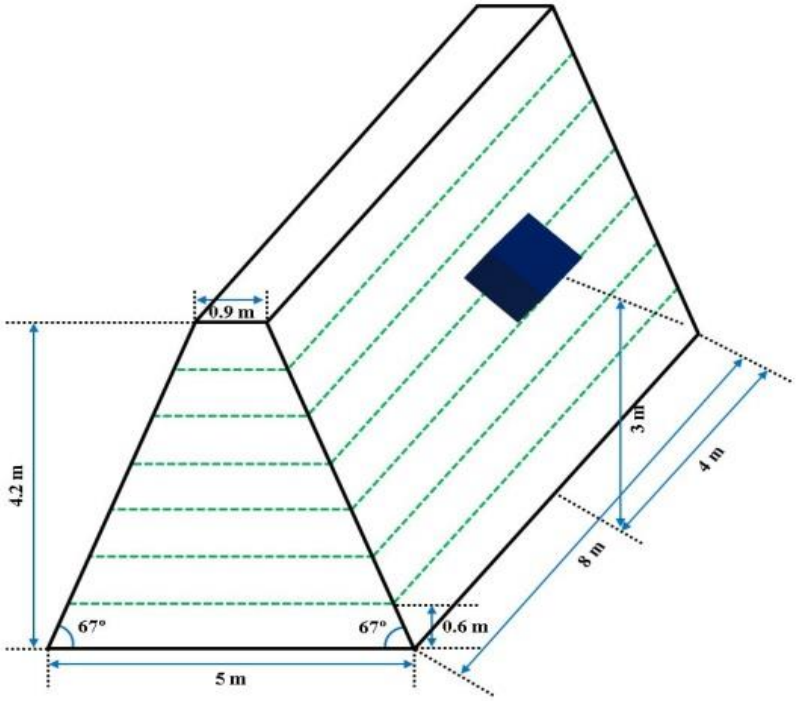

Fig. 1 The geometry of the reinforced embankment with geogrid and the block impact position in the practical test to use in modeling

Table 2 Characteristics of the impact test on reinforced protective embankment (Peila *et al*. 2007)

Test number	Block mass (Kg)	Block velocity (m/s)	Impact energy (KJ)
1	5000	31	2402
2	8700	31	4180

The geotechnical characteristics of the embankment and geogrid are given in Table 1. In this case, the soil is considered as a homogeneous and single-phase material without water. Also, the general characteristics of the performed tests and the kinetics parameters including, mass, speed, and energy, are listed in Table 2.

2.2 Construction of DEM model

The DEM modeling to study the motion and deformation of block/particle systems were developed progressively in the early 1970s (Cundall 2010). This study uses the discrete element method (DEM) to model and analyzes the reinforced embankment's stability with similar conditions to this practical test. For this purpose, YADE, as an open-source code based on DEM, has been used. The particle-based code YADE represents soils/rocks using glued discs/spheres and models the fracturing process based on the rupture of inter-particle bonds with the contact bond algorithms that elements each of them are spherical and corresponds to a rigid and homogeneous body that interacts with its neighbors at the contact points. The enhanced flexibility and improvement of results by adding new modeling capabilities are the main advantage of the developed models of YADE (Smilauer *et al.* 2010).

In this study, spherical and rigid elements in compacted soil and geogrid layers have been used to model the embankment. A three-dimensional DEM model developed for an embankment reinforced with geogrid under the impact of a rigid block shows in Fig. 2. A set of 65000 discrete elements were packed into the corresponding closed volume using a dynamic growth technique. According to this method, many non-contacting particles are randomly distributed inside the model with a uniform size distribution. In this research, the ratio between the maximum and the minimum radius of particles is chosen equal to 2. At this stage, the size of the particles is progressively increased until the model reaches an equilibrium state defined by the stabilization of its porosity over time.

2.3 Parameters set for this simulation

In work presented, particles are assumed to follow a linear elastic-plastic law which has proven to be well adapted to simulate cohesive-frictional materials. In this case, particles are bonded together by consistent integration of the contact forces for arbitrary movements of the objects, including sliding the contact point along the outer surface. So, high mechanical values were applied to avoid its crushing, according to the practical test of the considered rigid block. A linear elastic material model is used for the geogrid layer as reinforcement, and its properties are presented in Table 2.

Once the packing was generated, the model's boundary conditions were set by preventing the movements of the discrete element making up the boundary floor of the embankment. In this case, all other discrete elements could

Number of particles in each layer
3357
4648
5973
7492
8996
10262
12633

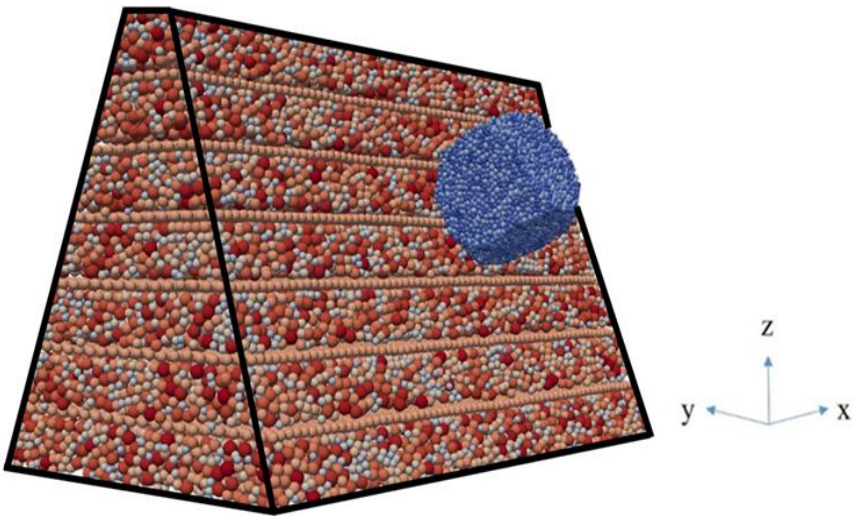

Fig. 2 Geometry of 3D-DEM model of block and embankment reinforced with geogrid

move in all directions. The gravity force was applied to the model before every simulation to generate in-situ stress and ensure embankment stability before impact.

Contact between soil layers and reinforcing elements is established by assuming a friction angle of 24°, equal to the average amount determined by shear tests on geogrid elements (Del Greco *et al*. 1994). Also, the contact of the block with soil is modeled with a friction angle of 22°, which equates to the amount is obtained from the results of the back analysis of previous studies in this regard (Mayne *et al*. 1984). It should be noted that in the embankment modeling, the steel mesh on the embankment is not considered because previous studies (Ronco *et al*. 2009) have shown that the role of this element in the dynamic impacts is not very significant.

Because the problem is solved explicitly in the method used, so the time step should be chosen correctly to prevent numerical instability. On the other hand, all elements are spherical and rigid and interact with their neighbors at the contact points. Therefore, in modeling, the forces between the elements are calculated according to their overlap and relative speed in the previous step. In this case, at each time step, the call detection algorithm determines all potential contacts for each element, and then the interaction forces are calculated using Newton's second law. At each time step, the contact detection algorithm establishes the list of potential contacts for each element. Then the interaction forces are calculated, solving Newton's second law of motion. A rolling resistance acting at contact points is also required to represent the shear behavior that occurs in granular soils. Thus, a moment law has been inserted into the model. Moreover, for impact loadings, additional dissipative laws are required. Here, a damage law and viscous damping have been chosen. To reduce the computational cost while keeping many elements, each of them is spherical and corresponds to a rigid and homogeneous body that interacts with its neighbors at the contact points. The interaction forces acting between elements depend on their overlap and relative velocity calculated at the previous time step.

Table 3 Input parameters representing the impact loading of the generic soil

Parameter	Unit	Value
Normal stiffness	MN/m^2	170
Shear stiffness	MN/m^2	35
Local friction angle	◦	17
Local cohesion	KPa	20
Coefficient of rolling stiffness	-	1.8
Coefficient of rolling elastic limit	-	1.8
Coefficient of damaging law in release mode	-	8
Coefficient of nonlinear viscous law	-	1

The calibration and validation of the model were undertaken for quasi-static conditions as well as for impact loadings. The quasi-static behavior was set up using triaxial test simulations of the filling material. During this step, the DEM models were calibrated until the model could reproduce the mechanical properties of the generic soil. The input parameters representing the impact loading of the generic soil are presented in Table 3.

3. Results and discussion

The optimal design of rockfall protection embankment to reduce any damage and deformation requires the consideration of the influence of characteristics of both the impacting block and the embankment structure. This is commonly done using numerical modeling, which can be considered the interaction between the block and the embankment based on the motion and impact laws. This section presents the results obtained from the numerical modeling of block's impact to the embankment with two types of kinetic energy.

3.1 Modeling results of low-energy impact

In this section, the results of block impact with the

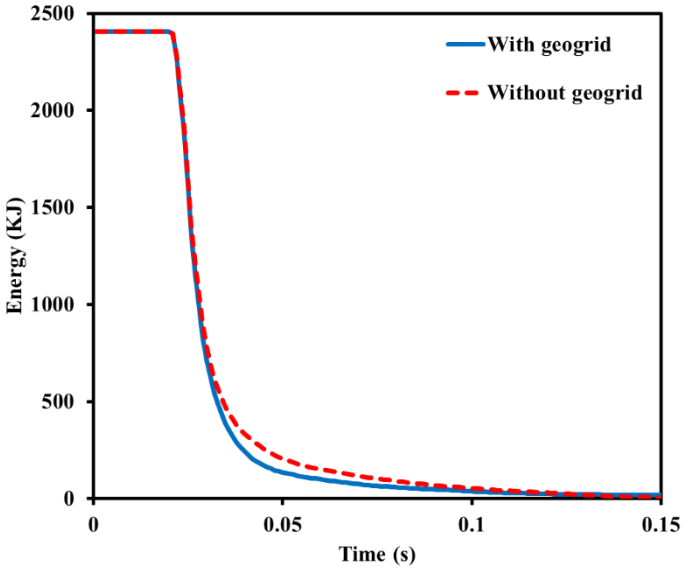

Fig. 3 Reduction of kinetic energy over time due to blocks' impact with the energy of 2402 KJ on the embankment reinforced with geogrid (solid blue curve) compared to unreinforced embankment (dashed red curve)

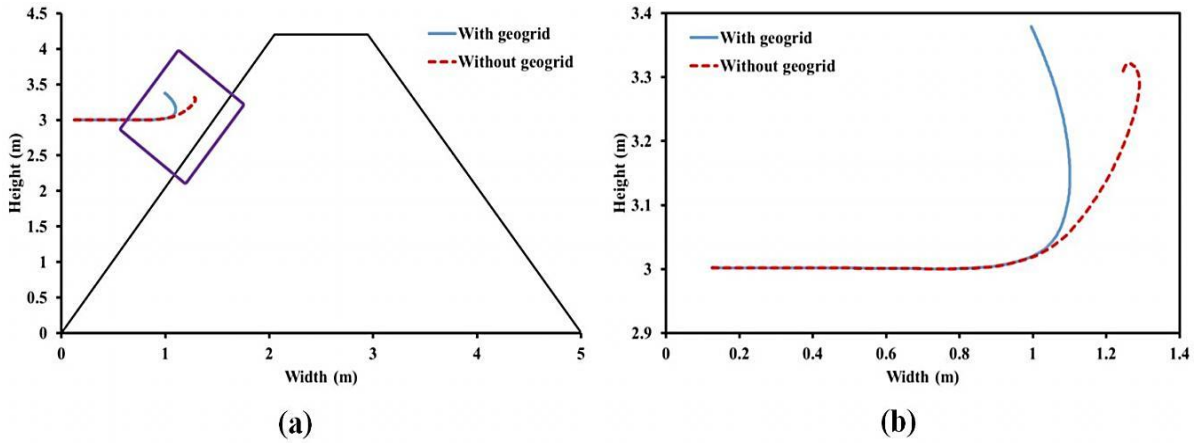

Fig. 4 Comparison of the movement path (a), and magnified penetration path (b) of block with energy of 2402 KJ due to impact to two reinforced with geogrid and unreinforced embankments

kinetic energy of 2402 kJ to unreinforced embankments and reinforced with geogrid are presented. In general, the results of modeling show that due to the block's impact to the embankment, a hole is formed in its front side, which prevents the block from passing through the embankment, and as a result, the block is stopped. The curve of reducing the kinetic energy of block in relation to time in two types of the modeled embankment is shown in Fig. 3. According to this figure, the block is stopped in impact with the unreinforced embankment (dashed red curve) and the embankment reinforced by the geogrid (solid blue curve) during 0.13 and 0.15 seconds, respectively. Therefore, the reinforced embankment by the geogrid is able to absorb more energy than the embankment without reinforcement and stops the block faster.

The movement path and the block's penetration depth after impacting the embankment with the kinetic energy of 2402 KJ are shown in Fig. 4. The left figure (Fig. 4(a)) shows the block penetration on the embankment. The right figure (Fig. 4(b)) shows the magnified image of the block's path in the impact with embankment without reinforcement (dashed red curve) and the embankment reinforced with geogrid (solid blue curve). In this case, at the moment of block impact to the embankment, the block has a vertical upward and backward movement due to the embankment slope. This movement is only on the plane y-z and has almost no movement in the transverse direction of x. Also, the penetration depth of the block in the reinforced embankment is lower than the unreinforced embankment.

In the unreinforced embankment (Fig. 5), the block's penetration depth on the embankment's front side is 0.82 m, and the maximum protrusion of its back side is obtained equal to 0.46 m. on the other hand, in the embankment reinforced with geogrid (Fig. 6), the block's penetration depth on the embankment's front side is 0.58 m, and the maximum protrusion of its back face is obtained equal to 0.19 m. The comparison between the results shows the effect of the absence of geogrid on increasing the

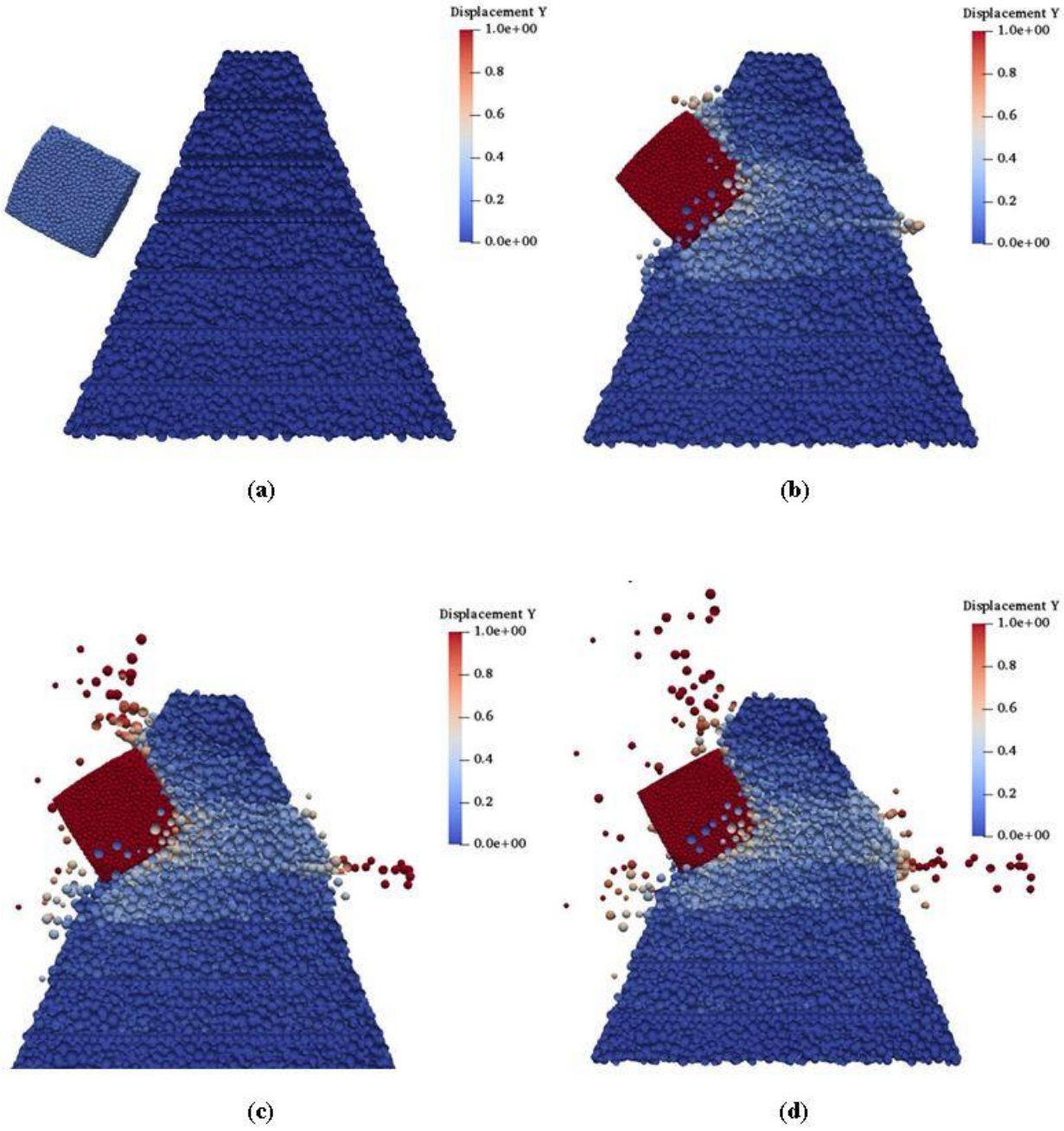

Fig. 5 Displacements of unreinforced embankment during impact of block with energy of 2402 KJ

penetration depth and protrusion. The results show that the walls reinforced with geogrid layers respond mainly by sliding on the surface where the geogrid is located. In this case, only a limited part of the whole structure (near the impact point) directly withstands the forces caused by the impact.

Also, the deformation of layers in the front (Figs. 7(b) and 7(d)) and back (Figs. 7(a) and 7(c)) sides of the unreinforced embankment (Figs. 7(a) and 7(b)) and the reinforced embankment with geogrid (Figs. 7(c) and 7(d)) due to the impact of the block with the energy of 2402 KJ is shown in Fig. 7, which confirms the decrease of penetration and protrusion depth in the reinforced embankment compared to the unreinforced embankment.

3.2 Modeling results of high-energy impact

In this section also the results of block impact with the kinetic energy of 4180 kJ to unreinforced embankments and reinforced with geogrid are presented. The curve of reducing the kinetic energy of block in relation to time in two types of the modeled embankment is shown in Fig. 8. According to this figure, the block is stopped in impact with the unreinforced embankment (dashed red curve) and the embankment reinforced by the geogrid (solid blue curve) during 0.18 and 0.2 seconds, respectively. In this case, the reinforced embankment can absorb more energy than the embankment without reinforcement and stops the block faster, but the stop time of the block is longer compared to the previous state (Fig. 3).

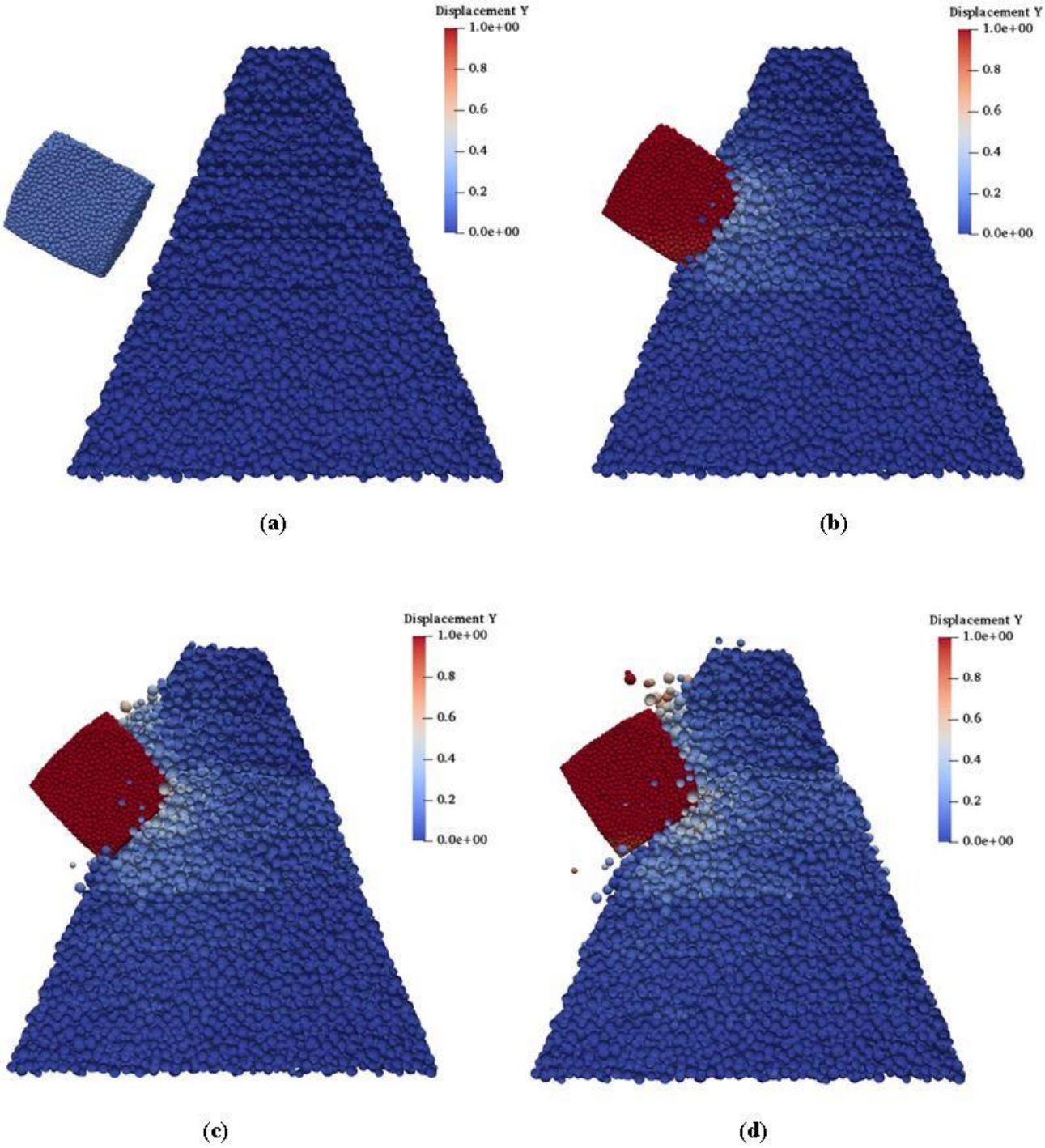

Fig. 6 Displacements of embankment reinforced with geogrid during impact of block with energy of 2402 KJ

In Fig. 9 also the movement path and the penetration depth of the block after impacting the embankment with the kinetic energy of 4180 KJ is shown. Similar to Fig. 4, the left figure (Fig. 9(a)) shows the amount of block penetration on the embankment, and the right figure (Fig. 9(b)) shows the magnified image of the path of the block in the impact with embankment without reinforcement (dashed red curve), and the embankment reinforced with geogrid (solid blue curve). A comparison between the block's penetration depth and its movement path after impacting the embankment in this case than before shows that blocks with more kinetic energy have more penetration depth. In this case, the block energy is used to move forward into the embankment, and the block has a downward movement in the unreinforced embankment.

In this case, the block's penetration depth on the embankment's front side is 1.29 m, and the maximum protrusion of its back side is obtained equal to 1.07 m in the unreinforced embankment (Fig. 10). Also, in the embankment reinforced with geogrid (Fig. 11), the block's penetration depth on the embankment's front side is 0.9 m, and the maximum protrusion of its back face is obtained

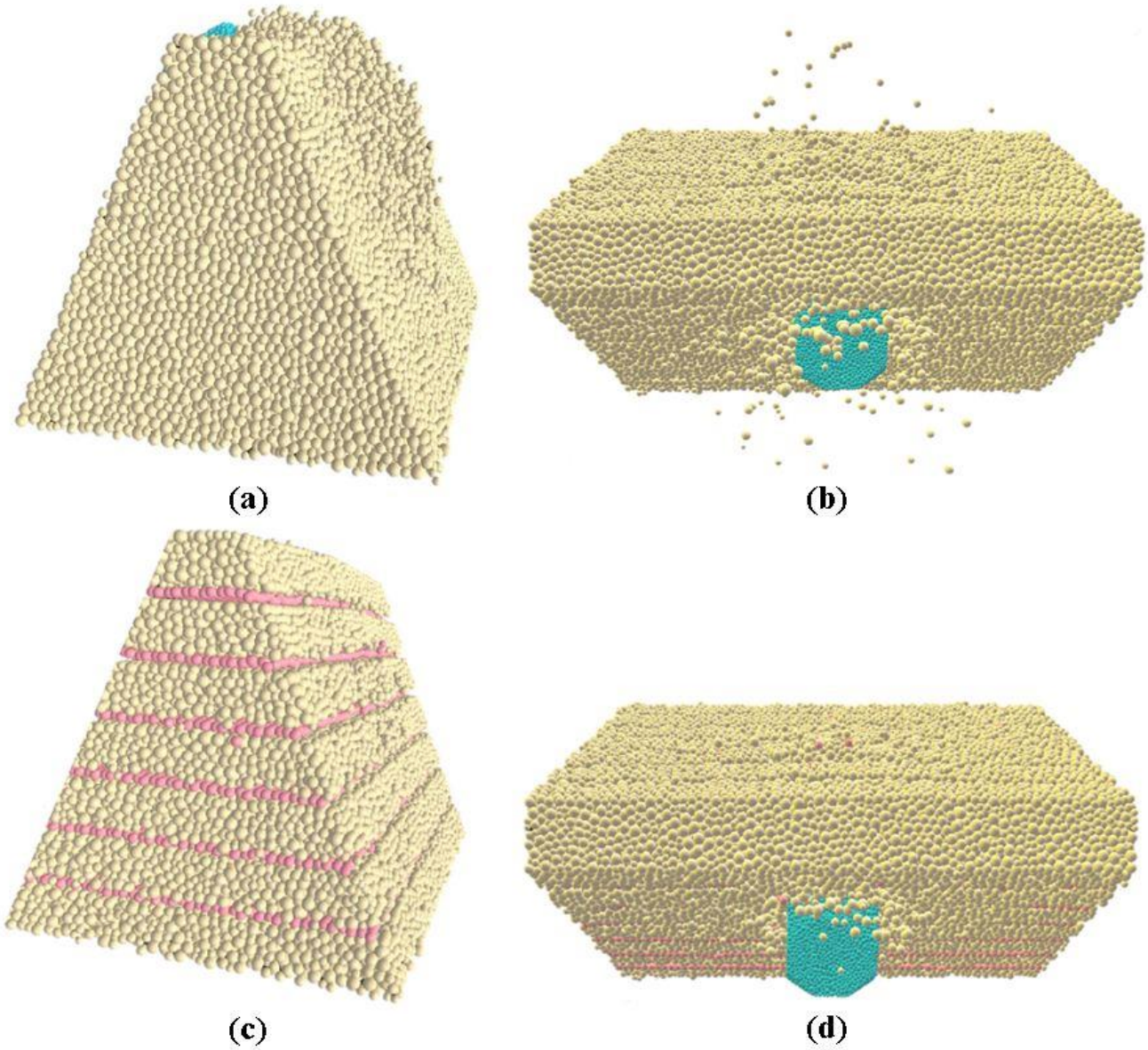

Fig. 7 Deformation of layers in the front (b), (d) and back (a), (c) sides of the unreinforced embankment (a), (b) and the reinforced embankment with geogrid (c), (d) due to the impact of block with energy of 2402 KJ

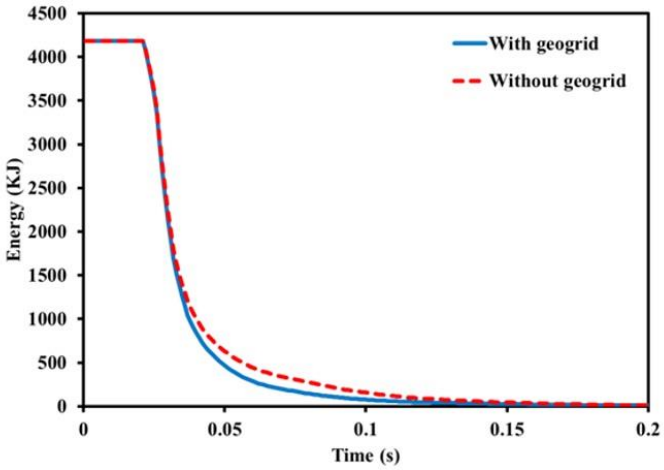

Fig. 8 Reduction of kinetic energy over time due to blocks' impact with the energy of 4180 KJ on the embankment reinforced with geogrid (solid blue curve) compared to unreinforced embankment (dashed red curve)

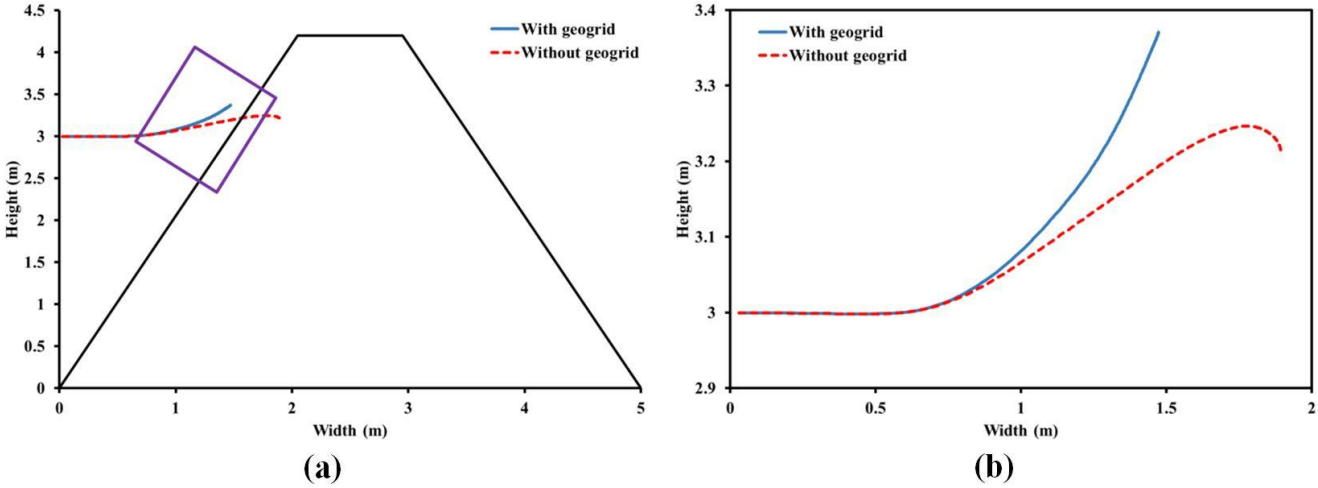

Fig. 9 Comparison of the movement path (a), and magnified penetration path (b) of block with energy of 4180 KJ due to impact to two reinforced with geogrid and unreinforced embankments

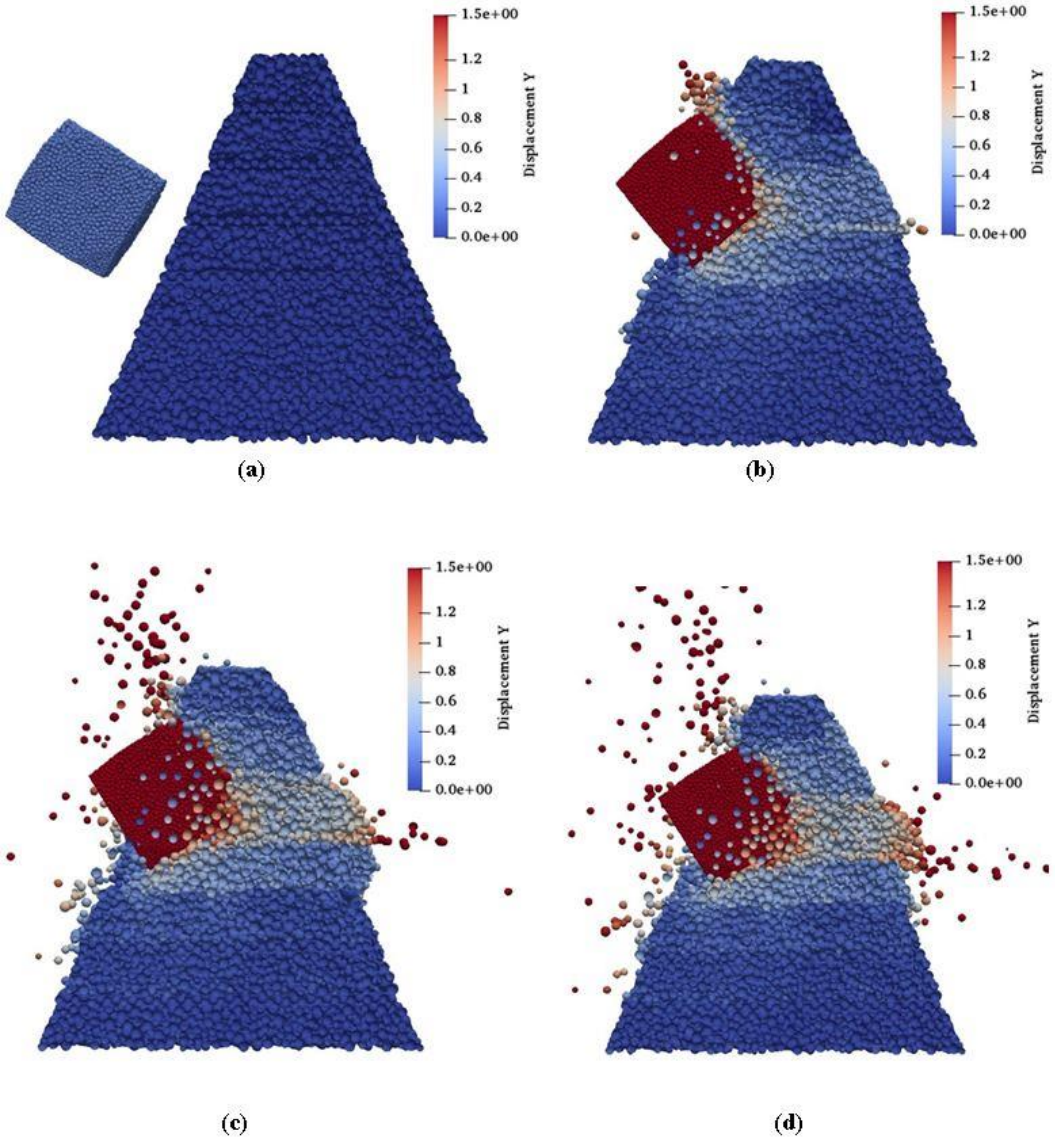

Fig. 10 Displacements of unreinforced embankment during impact of block with energy of 4180 KJ

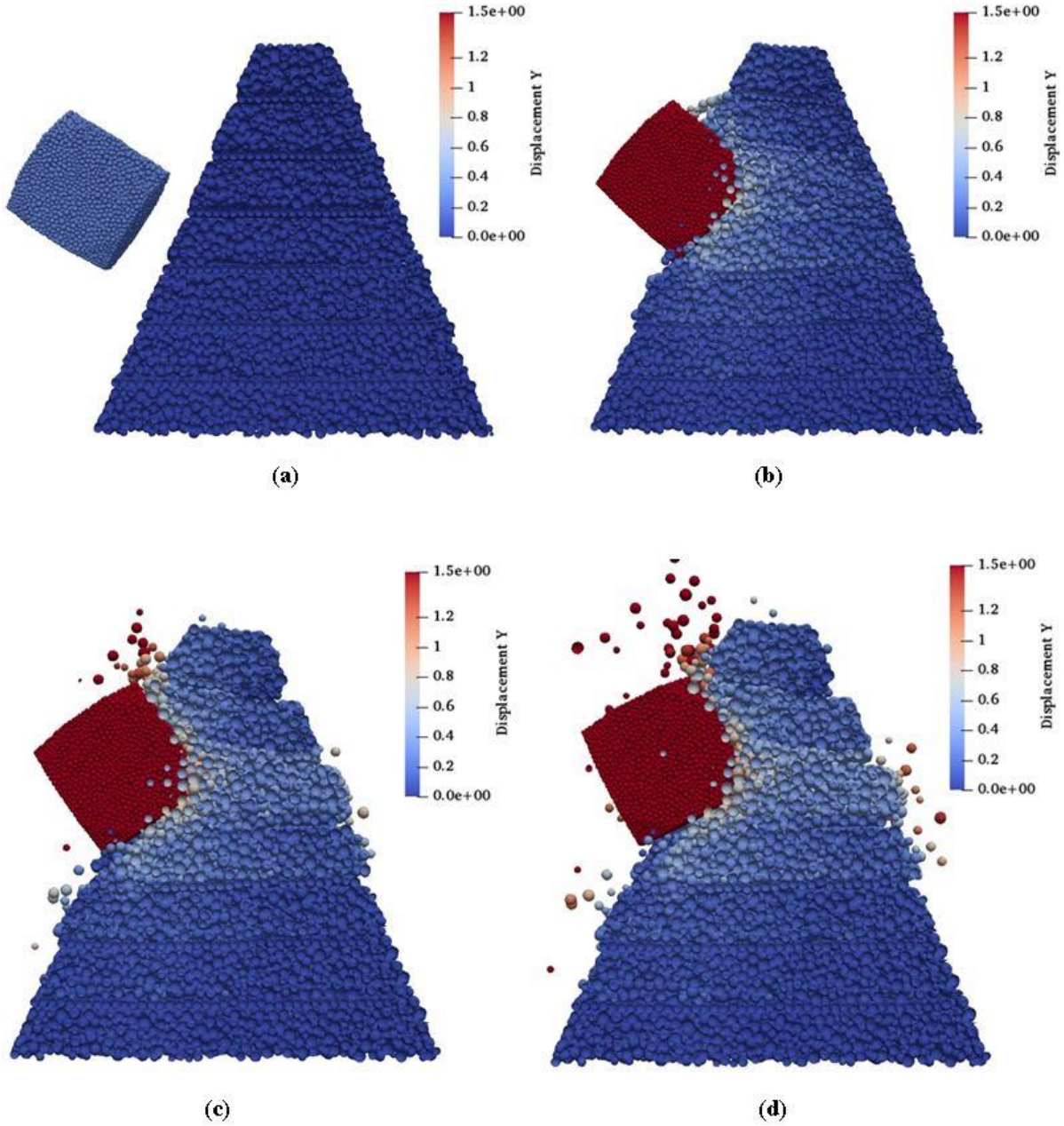

Fig. 11 Displacements of embankment reinforced with geogrid during impact of block with energy of 4180 KJ

equal to 0.7 m in the embankment reinforced with geogrid. The comparison between the results shows the effect of the absence of geogrid on increasing the penetration depth and protrusion.

Also the deformation of layers in the front (Figs. 12(b) and 12(d)) and back (Figs. 12(a) and 12(c)) sides of the unreinforced embankment (Figs. 12(a) and 12(b)) and the reinforced embankment with geogrid (Figs. 12(c) and 12(d)) due to the impact of the block with the energy of 4180 KJ is shown in Fig. 12. Comparison between these figures shows the effect of using geogrid in reducing the penetration depth and protrusion of the embankment; in addition, the embankment damage and the particles' movement are more significant than the previous state (low energy impact).

The maximum displacement obtained from the DEM modeling of rockfall in the front and back sides of embankments is summarized in Table 4. As can be seen from the last row of the table, the reduction percentage of penetration depth in the front side embankment and the protrusion of the back side of the embankment are at least 29.3% in two types of energy using the geogrid reinforced embankment. This percentage reduction in displacement caused by the impact of a block to the embankment indicates the proper performance of the geogrid layers to reinforce soils even in high-energy impact.

Also, in Table 5, the displacement values and percentage error in the front and back sides of the reinforced embankment with geogrid in the low and high energy of the block obtained from the analytical method and modeling by

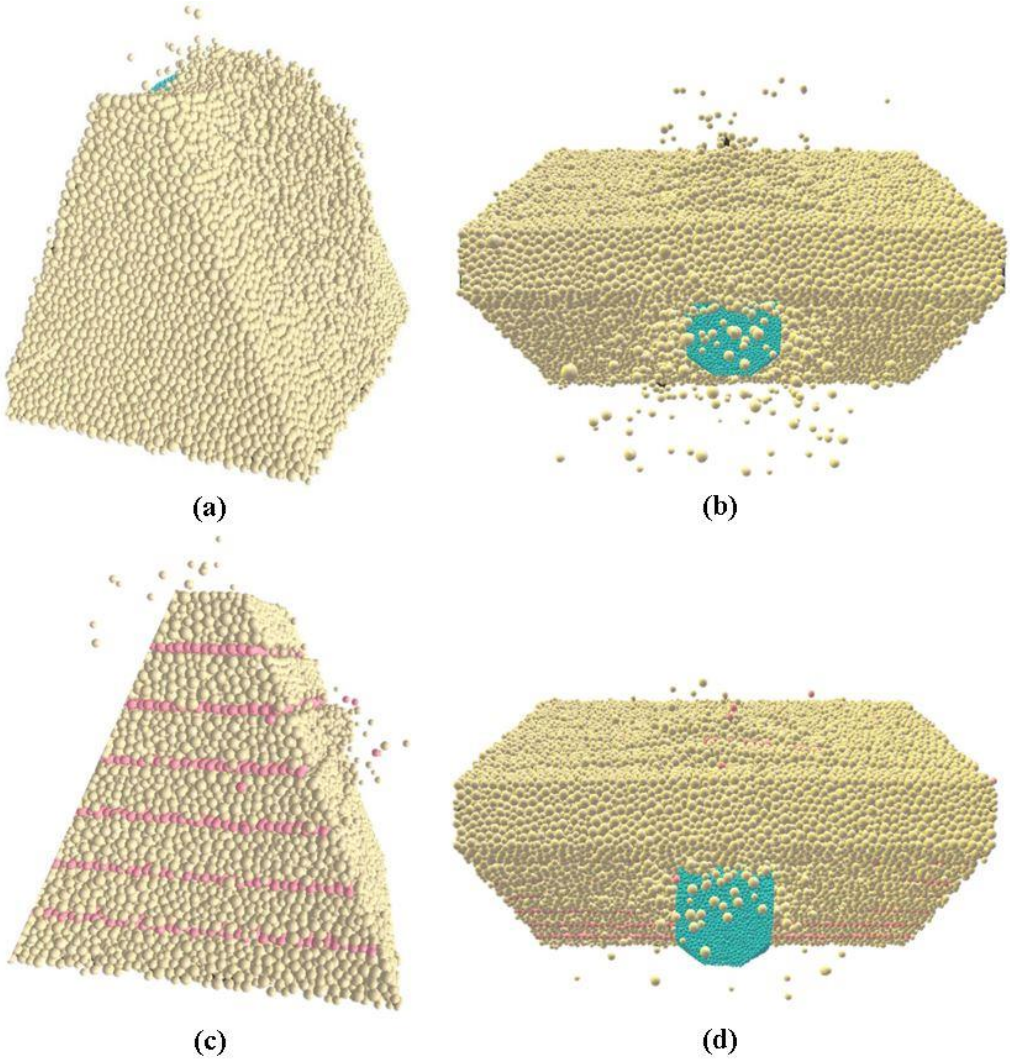

Fig. 12 Deformation of layers in the front (b), (d) and back (a), (c) sides of the unreinforced embankment (a), (b) and the reinforced embankment with geogrid (c), (d) due to the impact of block with energy of 4 KJ

FEM and DEM methods have been compared with the experimental test results. According to this table, in all cases, the displacement values obtained by the analytical method are higher than the large-scale experimental test.

The lowest percentage error calculated in this case is 63.3 %. Comparing the results of the two modeling methods shows that except for one case, namely the penetration depth in front of embankment under the low-energy impact, in almost all other cases, the percentage error of the DEM method was lower. The numerical results show that compared to the FEM method, the results of the model developed with DEM method in this study to investigate the performance of geogrid in the reinforcement of protective embankments is close to the results of large-scale experimental test. Therefore, using the procedure presented in this research, without performing costly and time-consuming practical tests, the optimal geogrid reinforced-soil embankments design can be achieved by constructing DEM models. This method can be used to study the strength and deformability behavior of geogrid layers inside embankments against rockfall.

Table 4 Displacement values of the unreinforced and reinforced with geogrid embankments

Embankment type	Block energy (KJ)			
	2402	4180	2402	4180
	Penetration in front side of embankment (m)		Protrusion in back side of embankment (m)	
Unreinforced embankment	0.82	1.29	0.46	1.07
Reinforced embankment with geogrid	0.58	0.9	0.19	0.7
Displacement reduction percentage (%) in reinforced embankment compared to unreinforced embankment	29.3	30.3	58.7	34.6

5. Conclusions

In this research, an attempt has been made to simulate the block's collision and evaluate the deformability of a protective embankment reinforced with geogrid by

Table 5 The percentage error of displacement obtained in different methods for the reinforced embankment with geogrid

Measurement method	Block energy (KJ)			
	2402	4180	2402	4180
	Penetration in front of embankment Value (m) Percentage error (%)		Protrusion in back of embankment Value (m) Percentage error (%)	
Experimental test (Peila *et al.* 2007)	0.6	0.95	0.17	0.8
Analytical method (Ronco *et al.* 2009)	0.22	0.26	0.04	0.06
	63.3 (%)	72.6 (%)	76.4 (%)	76.2 (%)
Numerical modeling with FEM (Peila *et al.* 2007)	0.38	0.95	0.2	0.5
	36.6 (%)	0 (%)	17.6 (%)	22.9 (%)
Numerical modeling with DEM	0.58	0.9	0.19	0.7
	3.3 (%)	5.2 (%)	11.7 (%)	8.2 (%)

numerical modeling using the discrete element method. For this purpose, firstly, 3D DEM numerical models of the unreinforced and reinforced embankments with geogrid have been made based on the data of a practical test on a real protective embankment. Then deformations due to the block's dynamic impact on the embankment, equivalent to the penetration depth of the block in the front side and protrusion of the back side of the embankment, have been determined. The results obtained in this study show that by using the embankment reinforced with geogrid, the displacement in the embankment's front and back is reduced by more than 29.3% compared to the unreinforced state. In fact, the geogrid layers prevent the slipping and movement of soil layers under the impact. Therefore, the reinforced embankment can absorb more energy than the embankment without reinforcement and stops the block faster. Also, in this case, the displacement obtained from the DEM modeling of the embankment reinforced with geogrid after impact was very close to the displacement measured from the large-scale experimental test. In this case, compared to the practical test, the percentage error of displacement has been obtained between 3.3% until 11.7%. However, the maximum percentage error obtained with the FEM and analytical methods was 36.6% and 76.4, respectively. Therefore, it can be concluded that numerical modeling by DEM is a powerful tool to study the deformability behavior of geogrid-reinforced embankment against natural disasters like rockfall, which can be used in engineering designs. In this regard, because in the continuous numerical methods such as FEM, the material flow, surfaces slip, and collapse processes that may occur during the impact of the block to the embankment are not well modeled, so in these cases by explicitly modeling of the particles of soil layers with using of the discontinuous numerical methods such as DEM, the limitations of continuous methods can be overcome to a large extent, and they can be used with more confidence to design of rockfall protection embankments.

The 3D-DEM modeling developed in this paper appears especially suitable for determining the local and global deformations of an embankment with and without reinforcement under the influence of low and high-impact collisions. By extending this work to real case studies, further investigation can be generated to evaluate the role of the different features of block collision in the deformations and stability of the embankment. Therefore, sensitivity analyses would be needed to identify the parameters most significantly affecting the stability of the embankment, taking into consideration the geometry and mechanical properties of the block and the embankment as well as the type of impact. Ongoing studies are currently done to take advantage of the current efforts to more accurately investigate the issues raised and the complexity of real rockfall protection embankments.

References

Bertrand, D., Nicot, F., Gotteland, P. and Lambert, S. (2005), "Modelling a geo-composite cell using discrete analysis", *Comput. Geotech.*, **32**(8), 564-577. https://doi.org/10.1016/j.compgeo.2005.11.004.

Bourrier, F., Lambert, S., Heymann, A. and Gotteland, P. (2010), "Evaluation of the efficiency of a model of rockfall protection structures based on real-scale experiments", *Numer. Method. Geotech. Eng*., 441-446.

Burroughs, D.K., Henson, H.H. and Jiang, S.S. (1993), "Full scale geotextile rock barrier embankment testing, analysis and prediction". *Proceedings of the Geosynthetics*, Vancouver, Canada.

Calvetti, F. (1998), "Distinct element evaluation of the rock-fall design load for shelters", *Geotecnica*, **32**, 63-83.

Cantarelli, G., Giani, G.P., Gottardi, G. and Govoni, L. (2008), "Modelling rockfall protection fences", In the first world landslide forum.

Cazzani, A., Mongiovı, L. and Frenez, T. (2002), "Dynamic finite element analysis of interceptive devices for falling rocks", *Int. J. Rock Mech. Min. Sci*., **39**(3), 303-321. https://doi.org/10.1016/S1365-1609(02)00037-0.

Crosta, G.B. and Agliardi, F. (2004), "Parametric evaluation of 3D dispersion of rockfall trajectories", *Nat. Hazard. Earth Sys.*, **4**(4), 583-598. https://doi.org/10.5194/nhess-4-583-2004.

Cundall, P.A. (1971), "A computer model for simulating progressive, large-scale movement in blocky rock system", Proceedings of the international symposium on rock mechanics, Nancy, France.

Del Greco, O., Fornaro, M. and Oggeri, C. (1994), "Modification of a quarry face: Stabilisation criteria and environmental reclamation", *Proceedings of the 7th international congress IAEG*, Lisboa, Portugal.

Descourdes, F. (1997), "Rockfall", Publications of the Swiss Association for Soiland Rock Mechanics, 135.

Effeindzourou, A., Thoeni, K., Giacomini, A. and Wendeler, C. (2017), "Efficient discrete modelling of composite structures for rockfall protection", *Comput. Geotech*., **87**, 99-114. https://doi.org/10.1016/j.compgeo.2017.02.005.

Faisal Haji, A. (1993), "Field behaviour of a geogrid-reinforced slope", *Geotext. Geomembranes*, **12**(1), 53-72. https://doi.org/10.1016/0266-1144(93)90036-N.

Kar, A.K. (1978), "Projectile penetration into buried structures", *J. Struct. Division*, **104**(1), 125-139. https://doi.org/10.1061/JSDEAG.0004814.

Kister, B. and Fontana, O. (2011), "On the evaluation of rockfall

parameters and the design of protection embankments-a case study", *Proceeding of the Interdisciplinary Workshop on Rockfall Protection-Rocexs*, Innsbruck, Austria.

Labiouse, V., Descoeudres, F. and Montani, S. (1996), "Experimental study of rock sheds impacted by rock blocks", *Struct. Eng. Int.*, **6**(3), 171-176. https://doi.org/10.2749/101686696780495536.

Lambert, S. and Bourrier, F. (2013), "Design of rockfall protection embankments: a review", *Eng. Geol.*, **154**, 77-88. https://doi.org/10.1016/j.enggeo.2012.12.012.

Lambert, S., Gotteland, P. and Nicot, F. (2009), "Experimental study of the impact response of geo-cells as components of rockfall protection embankments", *Nat. Hazard. Earth Sys.*, **9**(2), 459-467. https://doi.org/10.5194/nhess-9-459-2009.

Lambert, S. and Kister, B. (2017), "Analysis of existing rockfall embankments of Switzerland (AERES) Part A: State of knowledge", Technical report, 55.

Lazzari, A., Troisi, C. and Arcuri, G. (1996), "Protezione di nuclei abitati contro la caduta di massi mediante rilevati in terra rinforzata: esperienze della Regione Piemonte", *Proceedings of the Giornata di Studio su La protezione contro la caduta di massi dai versanti rocciosi*, Torino, Italy.

Maegawa, K., Tajima, T., Yokota, T. and Tohda, M. (2011), "Experiments on rockfall protection embankments with geogrids and cushions", *Int. J. Geomate*, **1**, 19-24. https://doi.org/10.21660/2011.1e.

Mayne, P.W., Jones Jr,J. S. and Dumas, J.C. (1984), "Ground response to dynamic compaction", *J. Geotech. Eng.*, **110**(6), 757-774. https://doi.org/10.1061/(ASCE)0733-9410(1984)110:6(757).

Meng, Q., Xue, H., Song, H., Zhuang, X. and Rabczuk, T. (2023), "Rigid-block DEM modeling of mesoscale fracture behavior of concrete with random aggregates", *J. Eng. Mech.*, **149**(2), 04022114. https://doi.org/10.1061/JENMDT.EMENG-6784.

Moradi, G., Abdolmaleki, A., Soltani, P. and Ahmadvand, M. (2018), "A laboratory and numerical study on the effect of geogrid-box method on bearing capacity of rock-soil slopes", *Geomech. Eng.*, **14**(4), 345-354. https://doi.org/10.12989/gae.2018.14.4.345.

Moradi, G., Abdolmaleki, A. and Soltani, P. (2019), "Small-and large-scale analysis of bearing capacity and load-settlement behavior of rock-soil slopes reinforced with geogrid-box method", *Geomech. Eng.*, **18**(3), 315-328. https://doi.org/10.12989/gae.2019.18.3.315.

Oggeri, C., Peila, D. and Recalcati, P. (2004), "Rilevati paramassi", *Proceedings of the Convegno Bonifica di versanti rocciosi per la protezione del territorio*, Trento, Italy.

Ouyang, C., Liu, Y., Wang, D. and He, S. (2019), "Dynamic analysis of rockfall impacts on geogrid reinforced soil and EPS absorption cushions", *KSCE J. Civil Eng.*, **23**(1), 37-45. https://doi.org/10.1007/s12205-018-0704-4.

Paronuzzi, P. (1989), "Criteri di progettazione di rilevati paramassi", *Geologia tecnica*, **1**, 23-41.

Pasqualotto, M., Hugonin, B. and Vagliasindi, B. (2005), "Rilevati in terra rinforzata a protezione dalla caduta massi in Val di Rhemes (AO)", *Geoingegneria Ambientale e Mineraria*, **114**(1), 55-67.

Pasqualotto, M., Peila, D. and Oggeri, C. (2004), "Prestazioni di un sistema di rilevati a scogliera soggetti and impatto di massi", *Proceedings of the Convegno Bonifica di versanti rocciosi per la protezione del territorio*, Trento, Italy.

Peckover, F.L. and Kerr, J.W.G. (1977), "Treatment and maintenance of rock slopes on transportation routes", *Can. Geotech. J.*, **14**(4), 487-507.

Peila, D., Castiglia, C., Oggeri, C., Guasti, G., Recalcati, P. and Rimoldi, P. (2002), "Testing and modelling geogrid reinforced soil embankments subject to high energy rock impacts", *Proceedings of the 7th International conference on geosynthetics*.

Peila, D., Oggeri, C. and Baratono, P. (2006), "Barriere paramassi a rete: interventi e dimensionamento", GEAM.

Peila, D., Oggeri, C. and Castiglia, C. (2007), "Ground reinforced embankments for rockfall protection: design and evaluation of full scale tests", *Landslides*, **4**(3), 255-265. https://doi.org/10.1007/s10346-007-0081-4.

Peila, D., Pelizza, S. and Sassudelli, F. (1998), "Evaluation of behaviour of rockfall restraining nets by full scale tests", *Rock Mech. Rock Eng.*, **31**(1), 1-24. https://doi.org/10.1007/s006030050006.

Peila, D. and Ronco, C. (2009), "Design of rockfall net fences and the new ETAG 027 European guideline", *Nat. Hazard. Earth Sys.*, **9**(4), 1291-1298. https://doi.org/10.5194/nhess-9-1291-2009.

Pichler, B., Hellmich, C. and Mang, H.A. (2005), "Impact of rocks onto gravel design and evaluation of experiments", *Int. J. Impact Eng.*, **31**(5), 559-578. https://doi.org/10.1016/j.ijimpeng.2004.01.007.

Plassiard, J.P., Donze, F.V. and Plotto, P. (2005), "High energy impact on embankments: a numerical discrete approach", Discrete Element Group for Risk Mitigation. https://doi.org/10.1201/9781439833780.ch86.

Plassiard, J.P. and Donze, F.V. (2009), "Rockfall impact parameters on embankments: A discrete element method analysis", *Struct. Eng. Int.*, **19**(3), 333-341. https://doi.org/10.2749/101686609788957874.

Plassiard, J.P. and Donze, F.V. (2010), "Optimizing the design of rockfall embankments with a discrete element method", *Eng. Struct.*, **32**(11), 3817-3826. https://doi.org/10.1016/j.engstruct.2010.08.025.

Pol, A. and Gabrieli, F. (2021), "Discrete element simulation of wire-mesh retaining systems: An insight into the mechanical behavior", *Comput. Geotech.*, 134, 104076. https://doi.org/10.1016/j.compgeo.2021.104076.

Ronco, C., Oggeri, C. and Peila, D. (2009), "Design of reinforced ground embankments used for rockfall protection", *Nat. Hazard. Earth Sys.*, **9**(4), 1189-1199. https://doi.org/10.5194/nhess-9-1189-2009.

Simmons, M., Pollak, S. and Peirone, B. (2009), "High energy rock fall embankment constructed using a freestanding woven wire mesh reinforced soil structure", *Proceedings of the 60th Highway Geology Symposium*, Buffalo, New York.

Šmilauer, V., Catalano, E., Chareyre, B., Dorofeenko, S., Duriez, J., Gladky, A. and Thoeni, K. (2010), "Yade reference documentation", *Yade Documentation*, **474**(1). http://yade-dem.org/doc/.

Tissieres, P. (1999), "Ditches and reinforced ditches against falling rocks", *Proceedings of the Joint Japan-Swiss Scientific Seminar on Impact load by rock fall and design of protection structures*, Kanazawa, Japan, 4-7.

Tran, V.D.H., Meguid, M.A. and Chouinard, L.E. (2015), "Three-dimensional analysis of geogrid-reinforced soil using a finite-discrete element framework", *Int. J. Geomech.*, **15**(4), 04014066. https://doi.org/10.1061/(ASCE)GM.1943-5622.0000410.

Volkwein, A. (2005), "Numerical simulation of flexible rockfall protection systems", *Comput. Civil Eng.*, 1-11. https://doi.org/10.1061/40794(179)122.

Watanabe, T., Masuya, H., Satoh, A. and Nakamura, S. (2011), "Analysis of impact response of sand cushion for rockfall by distinct element method", *Appl. Mech. Mater.*, **82**, 92-99. https://doi.org/10.4028/www.scientific.net/AMM.82.92.

Wyllie, D.C. and Norrish, N.I. (1996), "Stabilization of rock slopes", Landslides Investigations and Mitigation, **247**, 474-506.

Yan, J., Chen, J., Tan, C., Zhang, Y., Liu, Y., Zhao, X. and Wang, Q. (2023), "Rockfall source areas identification at local scale by integrating discontinuity-based threshold slope angle and rockfall trajectory analyses", *Eng. Geol*., **313**, 106993. https://doi.org/10.1016/j.enggeo.2023.106993.

Yoshida, H. (1999), "Recent experimental studies on rockfall control in Japan", *Proceedings of the Joint Japan-Swiss Scientific Seminar on Impact load by rock fall and design of protection structures*, Kanazawa, Japan.

Zhu, C., He, M.C., Karakus, M., Zhang, X.H. and Guo, Z. (2021), "The collision experiment between rolling stones of different shapes and protective cushion in open-pit mines", *J. Mountain Sci.*, **18**(5), 1391-1403. https://doi.org/10.1007/s11629-020-6380-0.

Zhu, C., He, M., Tao, Z., Meng, Q. and Zhang, X. (2021), "Recognition and prevention of rockfall vulnerable area in open-pit mines based on slope stability analysis", *Geomech. Eng*., **26**(5), 441-452. https://doi.org/10.12989/gae.2021.26.5.441.

Zhu, C., He, M., Yin, Q., and Zhang, X. (2021), "Numerical simulation of rockfalls colliding with a gravel cushion with varying thicknesses and particle sizes", Geomech. Geophysics for Geo-Energy and Geo-Resources, **7**(11), 1-15. https://doi.org/10.1007/s40948-020-00203-8.

Zhu, C., Wang, D., Xia, X., Tao, Z., He, M. and Cao, C. (2018), "The effects of gravel cushion particle size and thickness on the coefficient of restitution in rockfall impacts", *Nat. Hazard. Earth Sys*., **18**(6), 1811-1823. https://doi.org/10.5194/nhess-18-1811-2018.

Zhu, Z.H., Yin, J.H., Qin, J.Q. and Tan, D.Y. (2019), "A new discrete element model for simulating a flexible ring net barrier under rockfall impact comparing with large-scale physical model test data", *Comput. Geotech*., **116**, 103208. https://doi.org/10.1016/j.compgeo.2019.103208.

CC